Supporting Information

Supramolecular AIE Polymer-based Rare Earth Metallogels for Selective Detection and High Efficiency Removal of Cyanide and Perchlorate

Qi Zhang[a], You-Ming Zhang*[a, b], Hong Yao[a], Tai-Bao Wei[a], Bingbing Shi[a] and Qi Lin*[a]

[a] *Key Laboratory of Eco-functional Polymer Materials of the Ministry of Education; Key Laboratory of Eco-environmental Polymer Materials of Gansu Province, College of Chemistry and Chemical Engineering, Northwest Normal University, Lanzhou, Gansu, 730070, China.*

[b] *Gansu Natural Energy Research Institute, Lanzhou, Gansu 730046, China.*

** Corresponding author.*

E-mail addresses: zhangnwnu@126.com (Y.-M. Zhang), linqi2004@126.com (Q. Lin).

Contents

1. Experimental section .....- 1 -

1.1 Chemicals and materials .....- 1 -

1.2 General Experimental Procedures.....- 1 -

2. Supplementary figures.....- 3 -

3. Supplementary table .....- 26 -

4.References .....- 28 -

1. Experimental section

1.1 Chemicals and materials

All solvents and reagents were commercially available in an analytical degree and used without further purification. All cations and anions were prepared in an aqueous solution (c = 0.1 m). ^{1}H NMR spectra were recorded at 600MHz and 400MHz, ^{13}C NMR spectra at 151MHz. Ultraviolet-visible (UV-vis) spectra were recorded on a Shimadzu UV-2550 spectrometer. Fluorescence emission spectra have been obtained using an RF-5301 / PC Optical spectro fluorophotometer (Shimadzu). Scanning Electron Micrographs (SEM) of xerogels were investigated using the JSM-6701F instrument with an acceleration voltage of 8 kV. The IR spectra were performed on a Digilab FTS-3000 Fourier transform-infrared spectrophotometer. A Rheological Properties Test was performed using a Rheolaser Lab Diffusing Wave Spectroscopy instrument (Rheolaser LAB 6 master, Formulaction, France). Dionex ICS-1500 ion chromatograph (Dionex, USA); DS6 conductivity detector; AERS 4mm anion suppressor; Chromeleon 6.8 chromatography workstation; IonPac AS22 anion analysis column (250 mm × 4 mm); IonPac AG22 anion protection column (50 mm ×4 mm).

1.2 General Experimental Procedures

^{1}H NMR Titration. PM (10 mg, 9.79 × 10^{-6} mol) was dissolved in DMSO-d_6 (0.5 mL). Then, a series of different equivalents of **TH** (0.5, 1.0, 1.5, equiv and so on) were added into the solution of **PM**, and their ^{1}H NMRs were recorded.

Fluorescence titration. (1). Fluorescence titration based on different concentrations cations: A serious of the **PT-G** gels with different concentrations (0.1 equiv., 0.2 equiv., 0.3 equiv., 0.4 equiv., and so on) metal ions (Eu^{3+} and Tb^{3+}) were prepared by dissolving **PM** (5 mg), **TH** (5 mg) and proper equivalent of metal salt in DMSO:H_2O (2:1/v:v) binary solution (0.3 mL). Then record their fluorescence intensity at 470 nm wavelength.

(2). Fluorescence titration based on different equivalent anions: The rare earth metallogels (**PT-GEu** and **PT-GTb**) with different equivalents (0.5 equiv., 1.0equiv., 1.5 equiv., 2.0 equiv., 2.5 equiv. and so on) of anions (ClO_4^- or CN^-) were prepared by dissolve **PT-GEu** or **PT-GTb** and proper equivalent of anions salt in DMSO:H_2O (2:1/v:v) binary solution (0.35 mL). Then record their fluorescence intensity at the 470 nm wavelength.

2. Supplementary figures

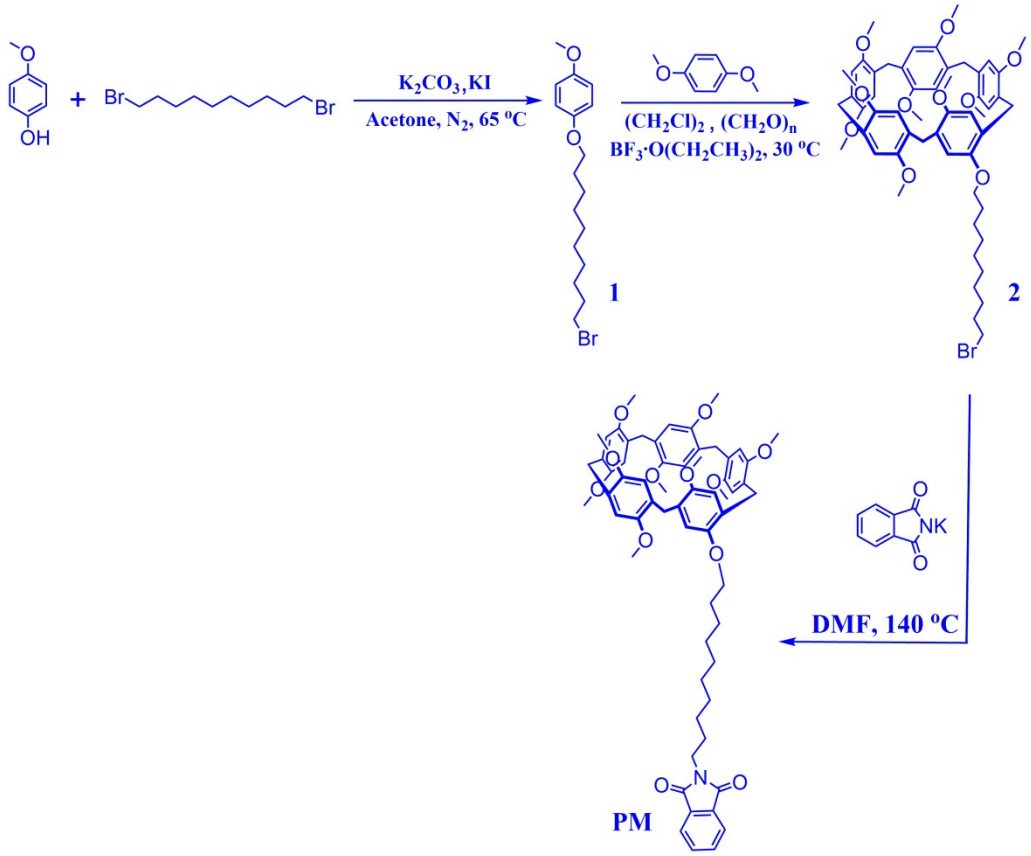

Scheme S1. Synthetic routes to compound **PM**.

Synthesis of the PM [1]**.** A mixture of pillar[5]arene (compound **2**) (1.1472g, 1.2 mmol) and *o*-phthalimide (0.46305g, 2.5 mmol) in DMF solution (35 mL) was stirred at 90 °C for 24 h under nitrogen atmosphere. The solution was evaporated under vacuum and the residue was purified by flash column chromatography (petroleum ether/ethyl acetate = 40/1, v/v) to afford **PM** as a yellow solid (0.996 g, 81.32%), mp: 60-62 °C. ^{1}H NMR (DMSO-d_6), 400 MHz), δ/ppm: 7.847-7.842 (m, 1H), 7.838- 7.833 (m, 1H), 7.712-7.707 (m, 1H), 7.703-7.698 (m, 1H), 6.796-6.763 (m, 10H), 3.843-3.821 (t, J = 6.5 Hz, 2H), 3.775-3.745 (m, 10H), 3.683- 3.650 (m, 27H), 3.646-3.643(t, J = 6.1 Hz, 2H), 1.773-1.657 (m, 4H), 1.488-1.320 (m, 2H), 1.307-1.228 (m, 10H). ^{13}C NMR (DMSO-d_6, 151 MHz), δ/ppm: 168.395, 150.643, 150.605, 133.818, 132.078, 128.258, 123.071, 114.820, 113.942, 68.463, 55.693, 53.191, 40.283, 40.141, 40.000, 39.723, 37.988, 29.692, 29.402, 29.061,

26.781, 26.213. MS m/z: $[PM]^+$ calcd for $C_{62}H_{71}NO_{12}$: 1021.4976; found: 1021.4968.

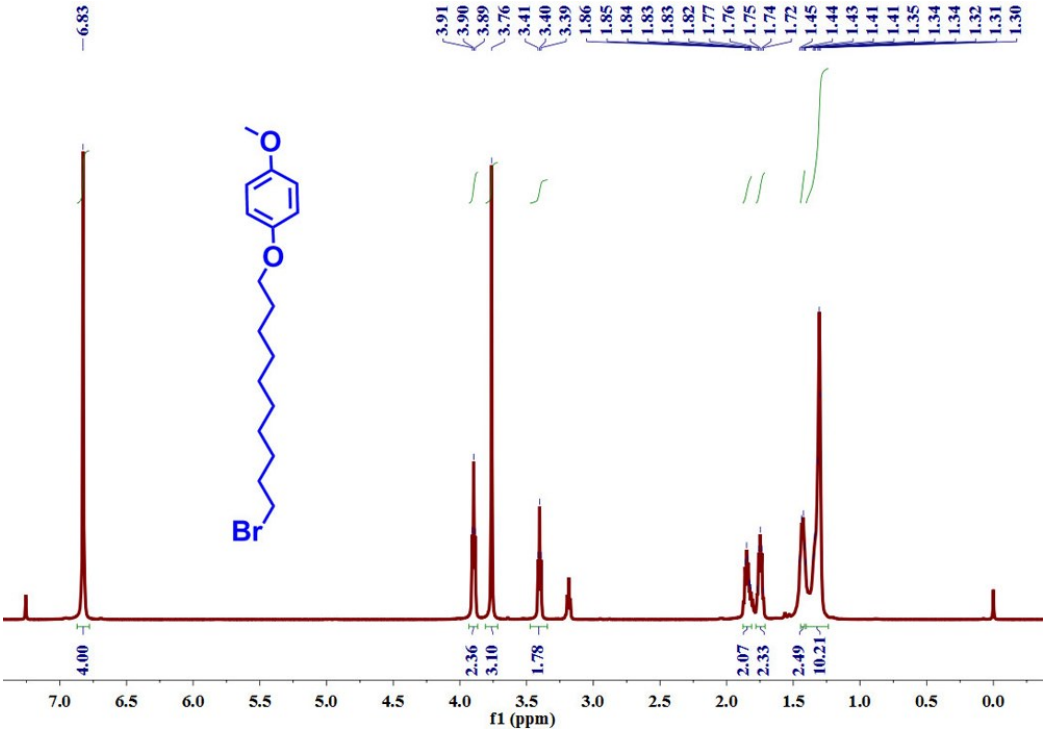

Figure S1. ^{1}H-NMR spectrum (600 MHz, $CDCl_3$) of compound **1**.

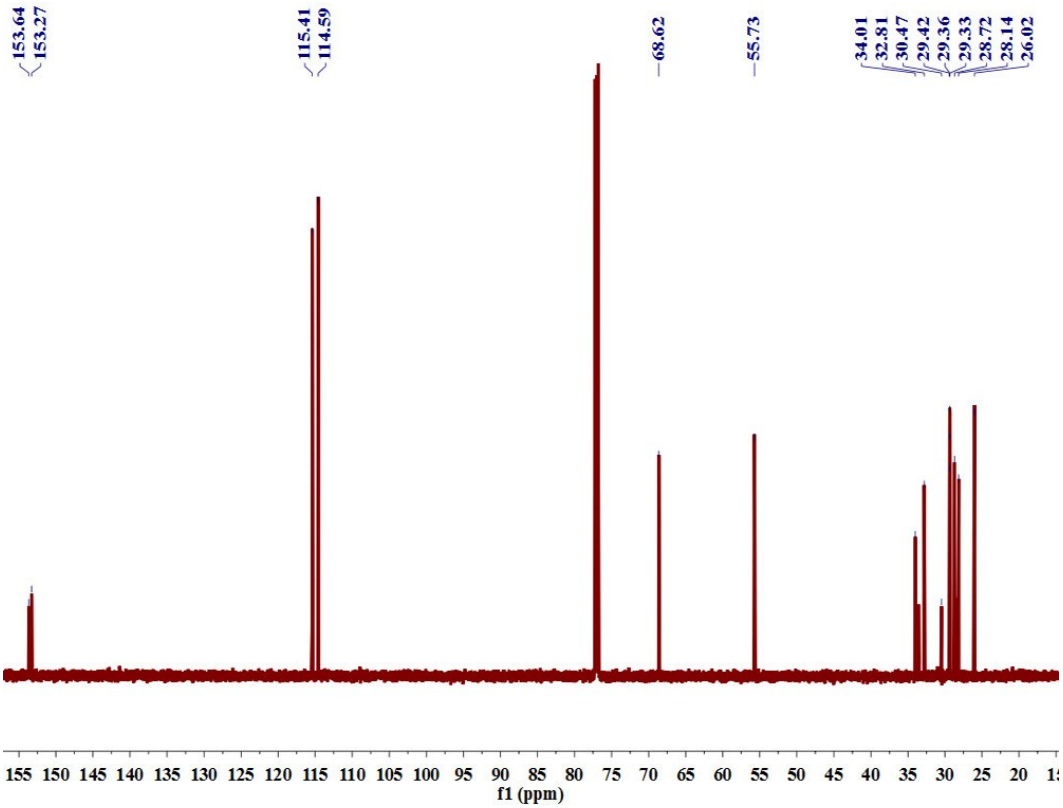

Figure S2. ^{13}C-NMR spectrum (151 MHz, $CDCl_3$) of compound **1**.

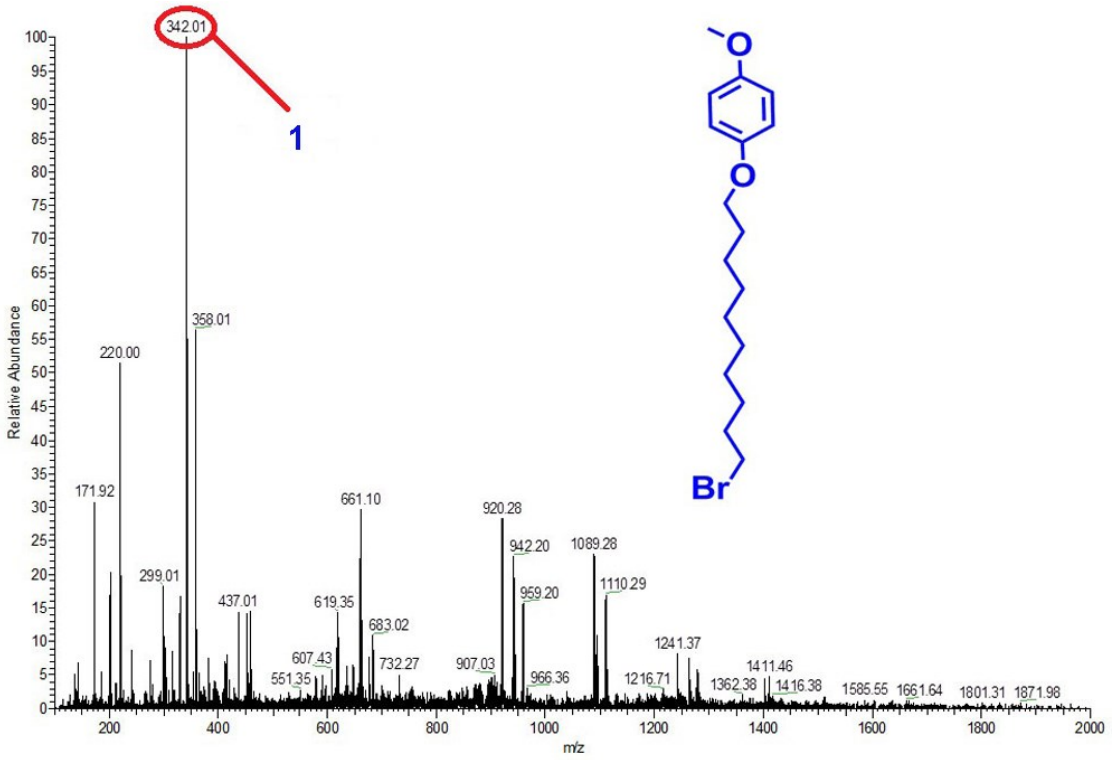

Figure S3. High resolution ESI-MS data of compound **1**.

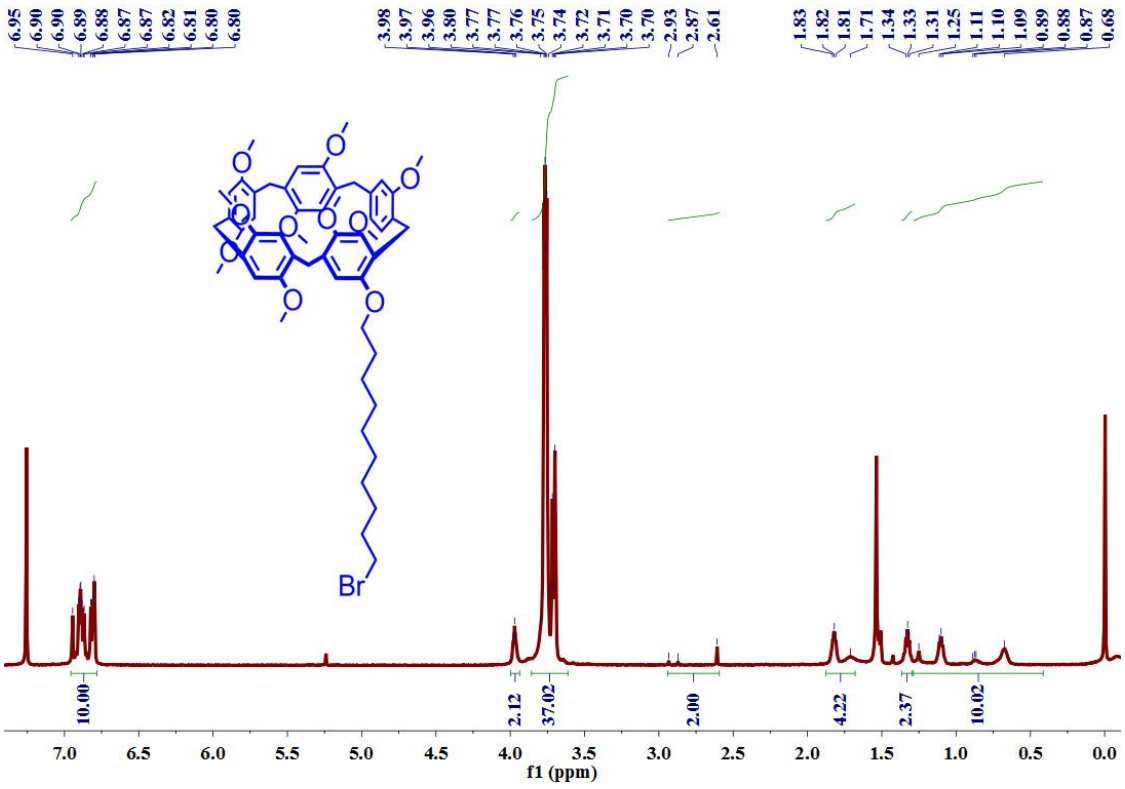

Figure S4. ^{1}H-NMR spectrum (600 MHz, $CDCl_3$) of compound **2**.

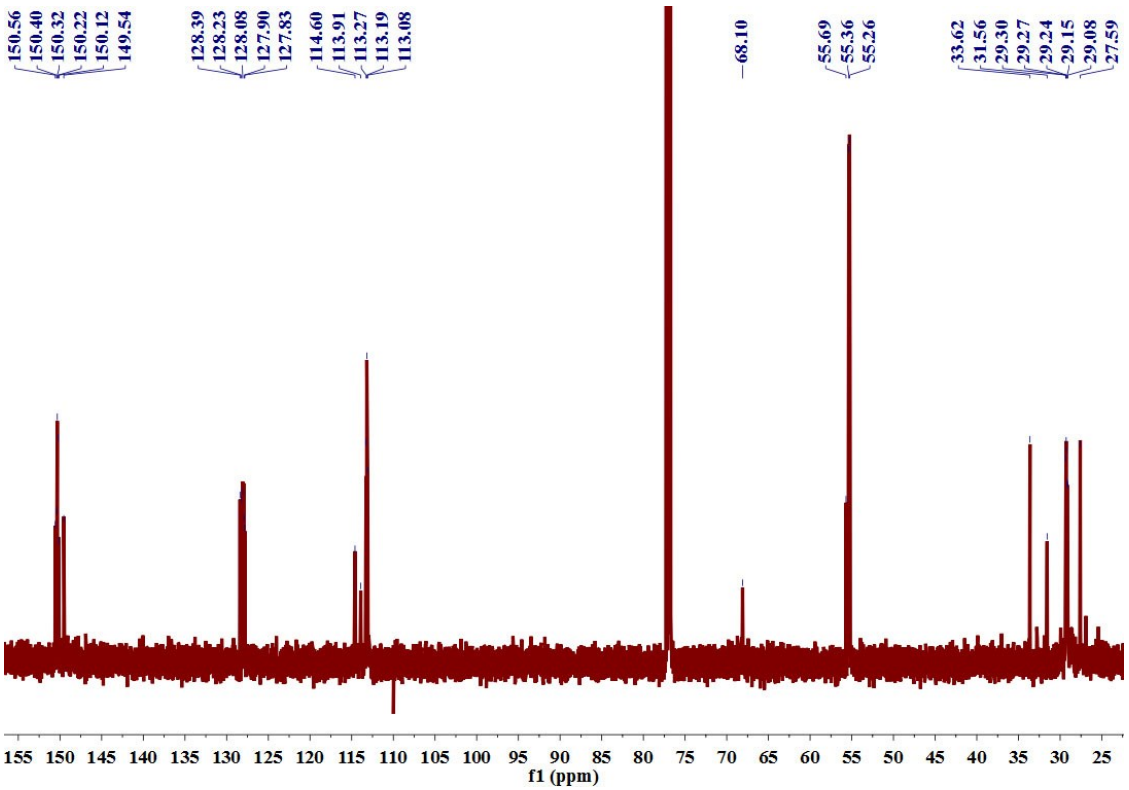

Figure S5. ^{13}C-NMR spectrum (151 MHz, $CDCl_3$) of compound **2**.

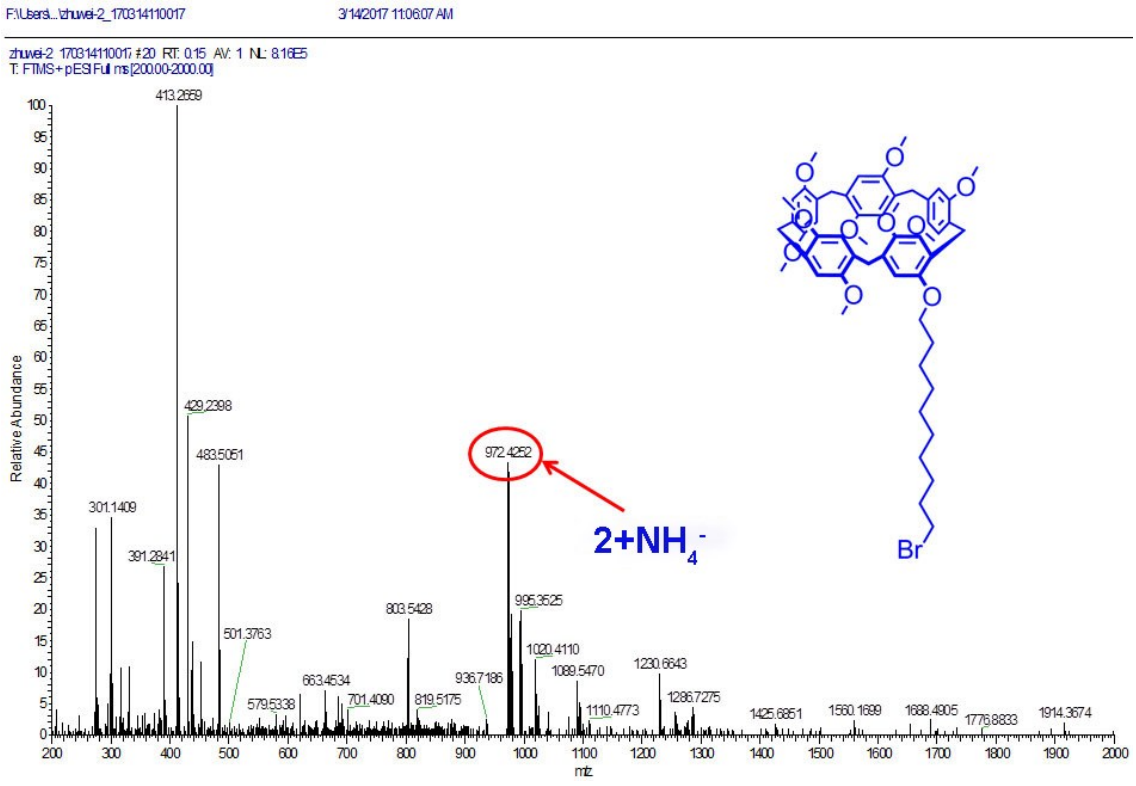

Figure S6. High resolution ESI-MS data of compound **2**.

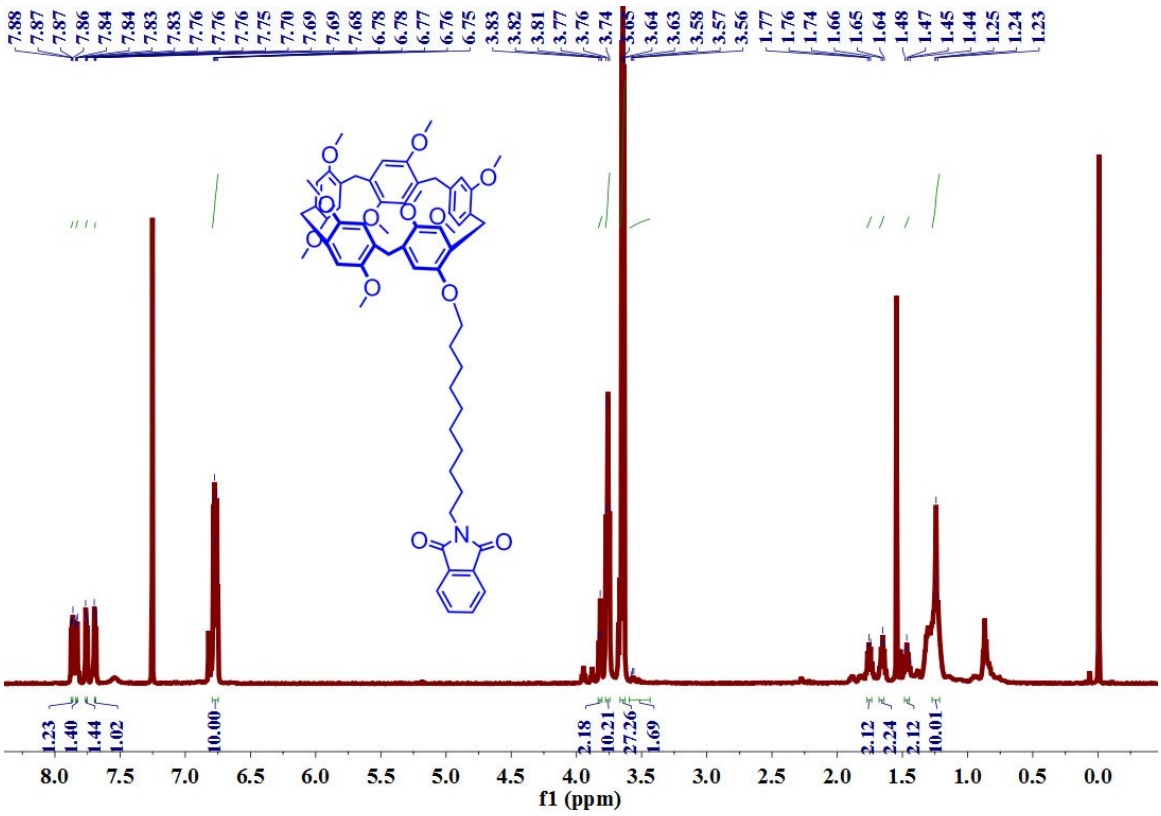

Figure S7. ^{1}H-NMR spectrum (600 MHz, DMSO-d_6) of compound **PM**.

Figure S8. ^{13}C-NMR spectrum (151 MHz, DMSO-d_6) of compound **PM**.

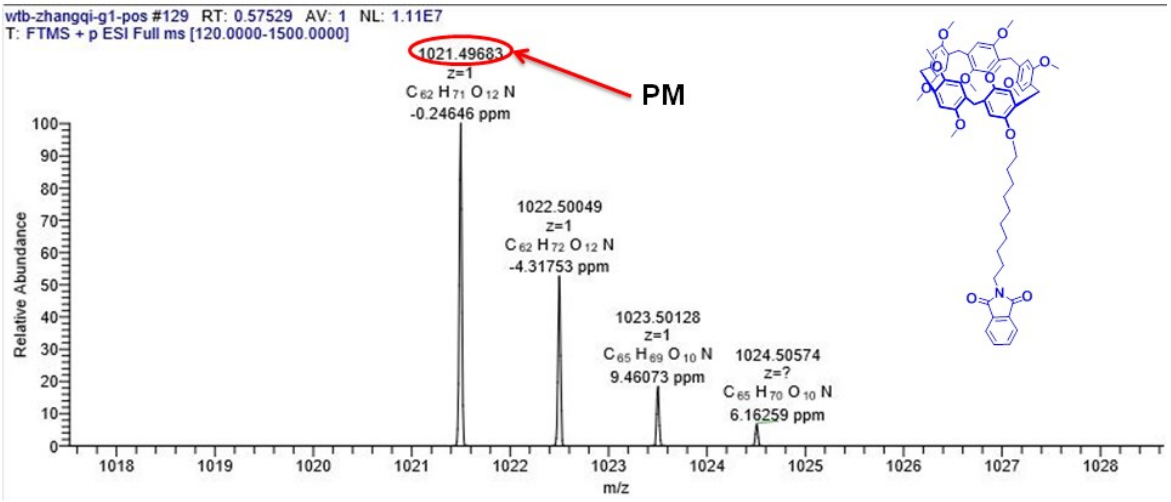

Figure S9. High resolution ESI-MS data of compound **PM**.

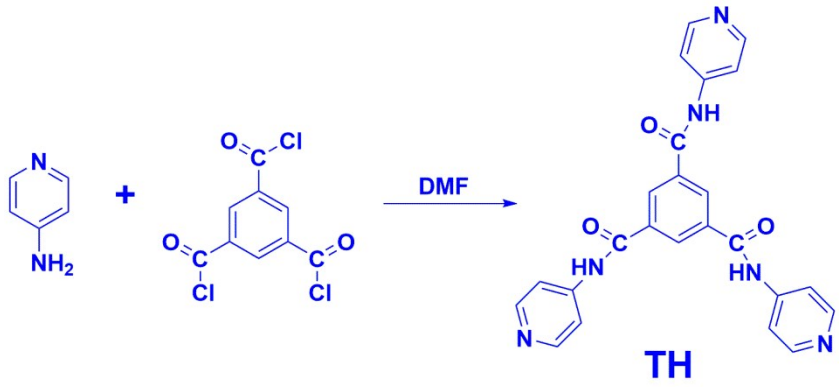

Scheme S2. Synthetic routes to compound **TH**.

Synthesis of the TH [2]**.** First, we put 1,3,5-benzenetricarbonyl trichloride (0.7965 g, 3.0 mmol) dissolution with DMF (20 mL), and then the solution was dropwise added to a mixture of 4-aminopyridine (1.1295 g, 11 mmol) and TEA (2 mL) in DMF (30 mL). The reaction mixture was stirred at room temperature for 24 h. Recrystallization of **TH** after the reaction was finished, then dried under vacuum. Yield: 0.7186 g (54.67%). M.p.: 270～272 ℃. ^{1}H NMR (400 MHz, DMSO-d_6), δ/ppm: 10.980 (s, 3H), 8.792-8.745 (t, J = 8.6 Hz, 3H), 8.457-8.519 (t, J = 5.4 Hz, 6H), 7.845-7.834 (t, J = 4.4 Hz, 6H). ^{13}C NMR (151 MHz, DMSO-d_6), δ/ppm: 166.05, 165.66, 150.87, 150.78, 146.26, 146.13, 145.41, 135.38, 134.92, 132.15, 131.03, 114.60, 109.24. MS m/z: [**TA** + H]$^{+}$ calcd for $C_{24}H_{19}N_6O_3$,

439.1519; found 439.1510.

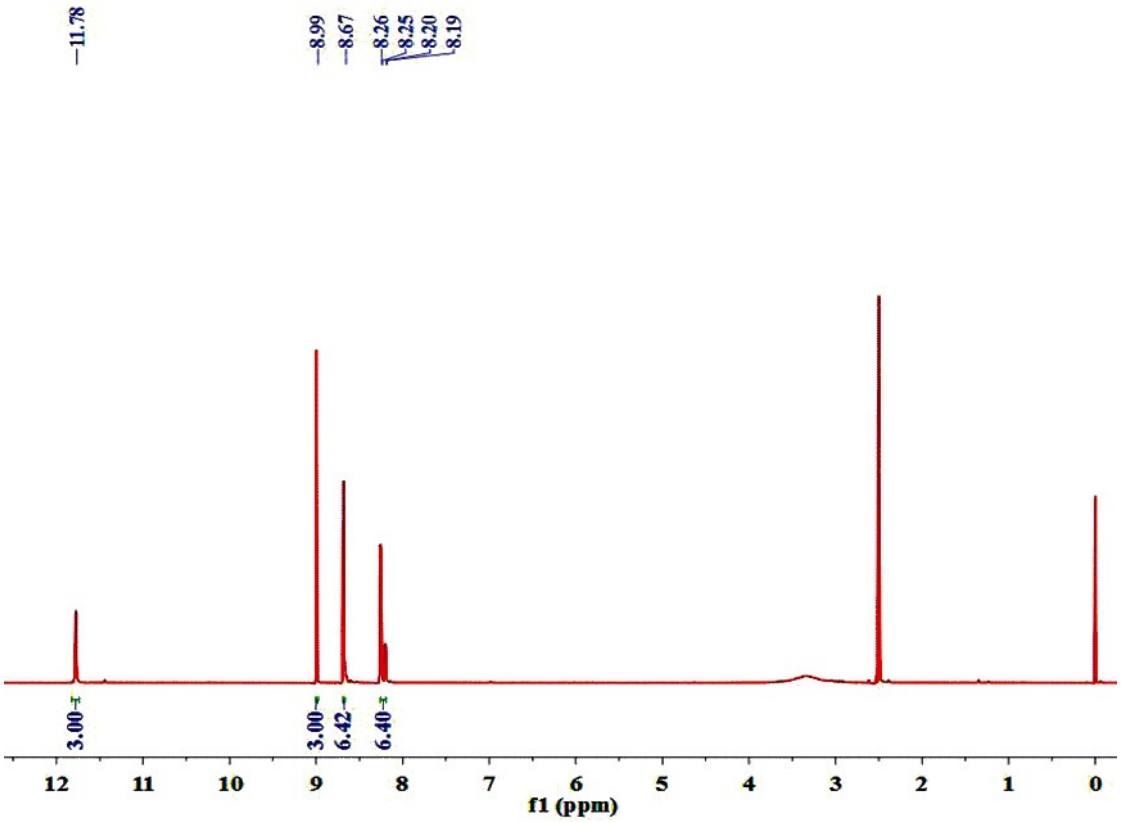

Figure S10. [1]H-NMR spectrum (600 MHz, DMSO-d_6) of compound **TH**.

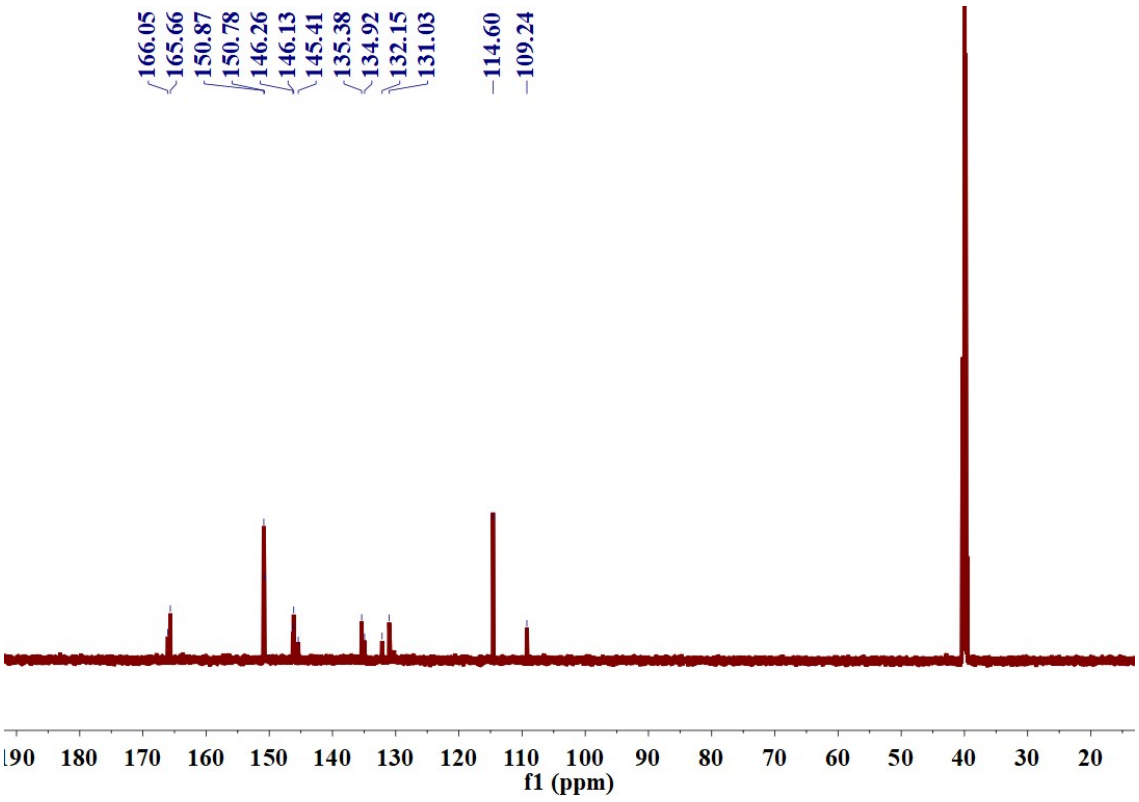

Figure S11. ^{13}C-NMR spectrum (151 MHz, DMSO-d_6) of compound **TH**.

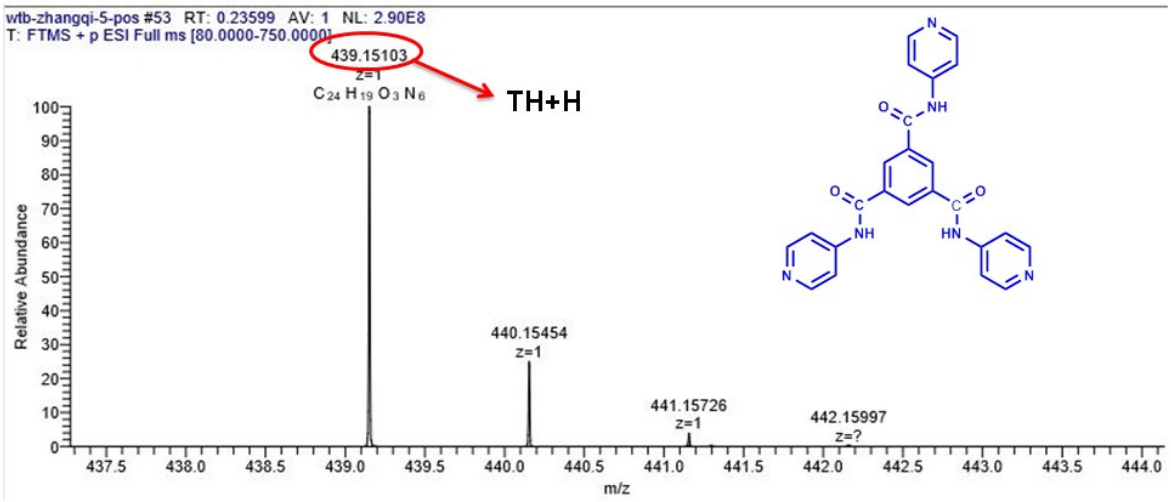

Figure S12. High resolution ESI-MS data of compound **TH**.

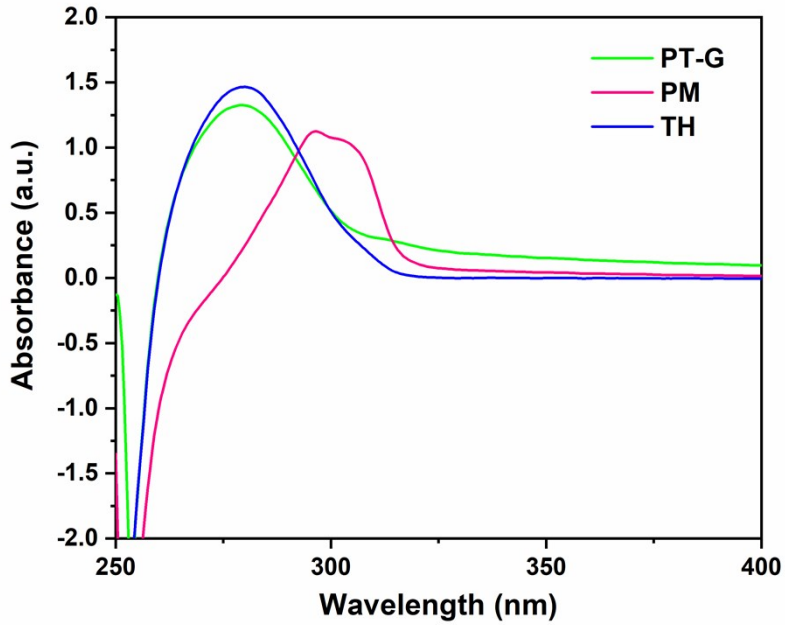

Figure S13. The UV-vis spectrum of the **PM**, **TH** and **PT-G** (2.0×10^{-5}M).

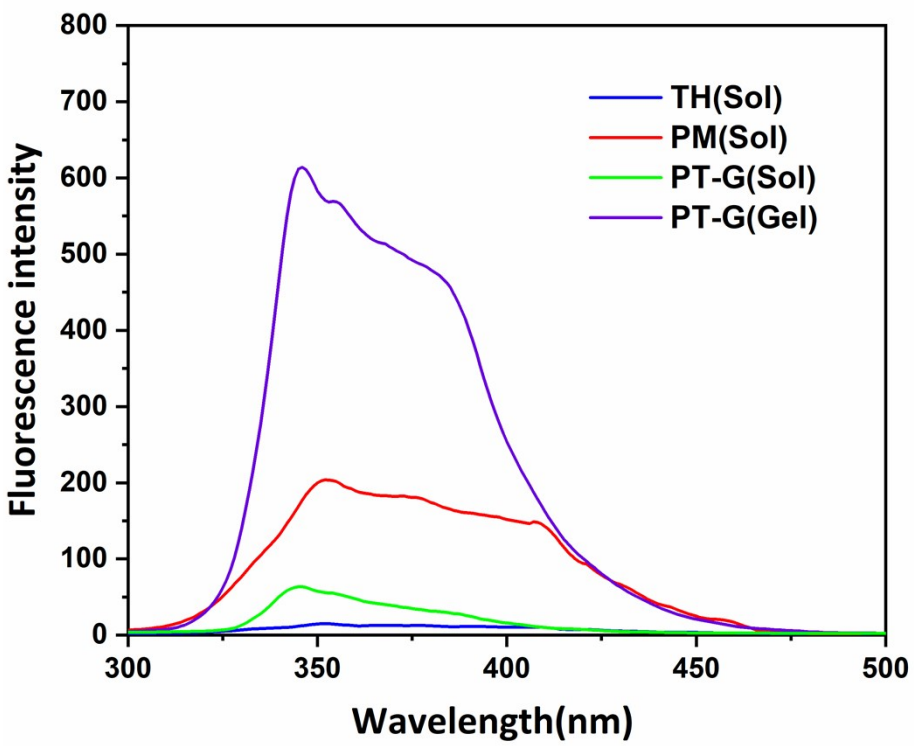

Figure S14. Fluorescence spectra of the DMSO-H_2O (2:1, v/v) binary solution of **PM** (c = 19 mM), **TH** (c = 19 mM), **PT-G** (c = 19 mM, T = 60°C > Tgel) and the **PT-G** gel (in the DMSO/H_2O (2:1, v/v) binary solution, c = 19 mM, T = 25 °C < Tgel).

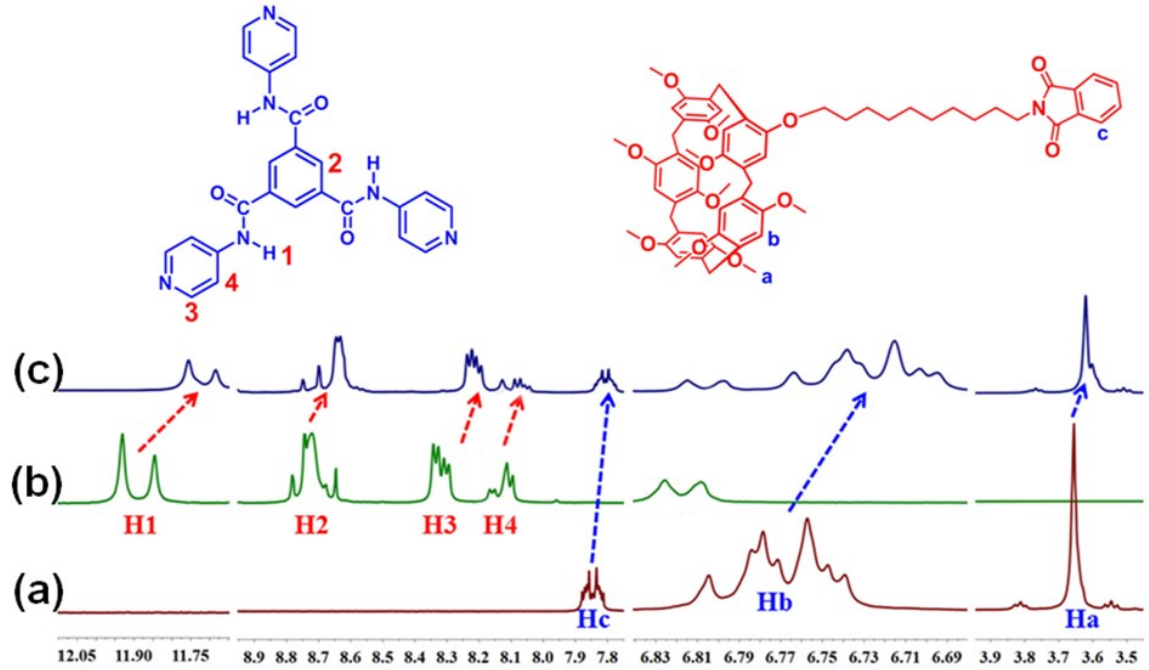

Figure S15. Partial host-guest 1H NMR spectra of (a) free PM, (b) free TH, (c) PM⊂TH 3.0 equiv. in (DMSO-d_6).

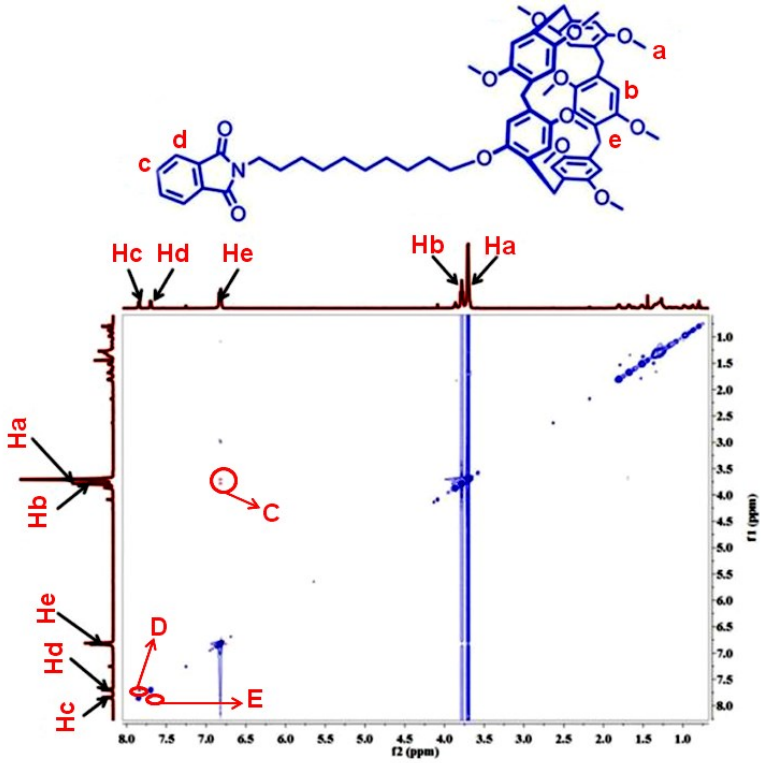

Figure S16. 2D-NOESY NMR spectrum of **PM** (10 mM**)** in $CDCl_3$ solution.

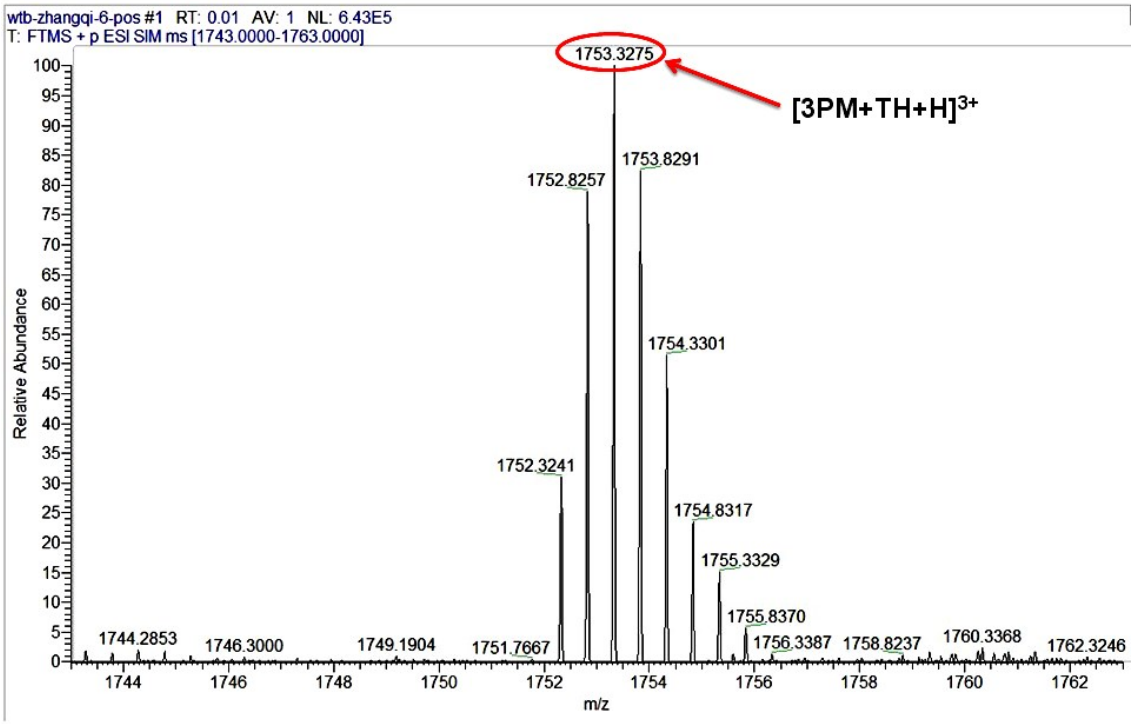

Figure S17. High resolution ESI-MS data of compound **PT-G**.

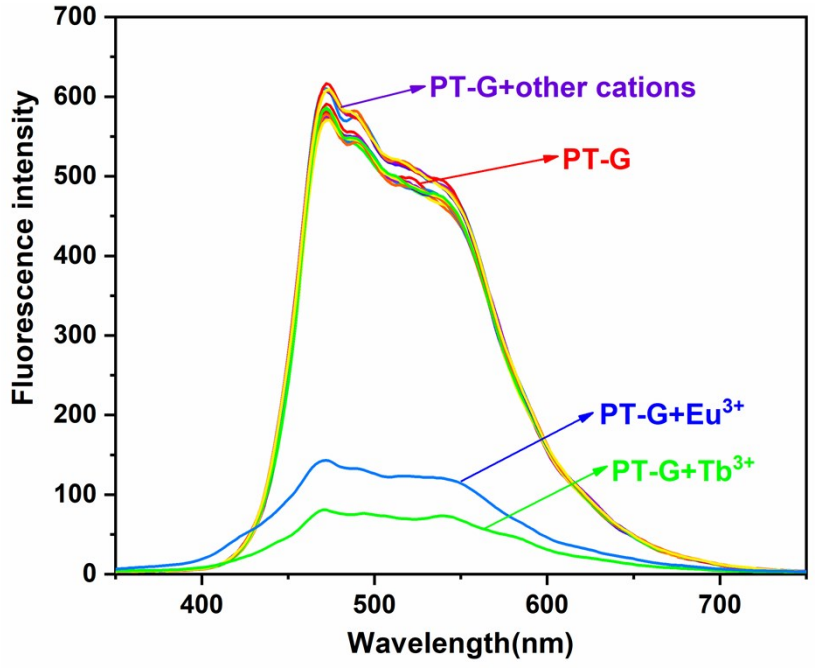

Figure S18. Fluorescence spectrum responses of the supramolecular gel **PT-G** (DMSO-H_2O (2: 1, v/v)) upon adding of various metal ions (Hg^{2+}, Ag^{+}, Ca^{2+}, Cu^{2+}, Co^{2+}, Ni^{2+}, Cd^{2+}, Pb^{2+}, Zn^{2+}, Cr^{3+}, Mg^{2+}, Ba^{2+}, Al^{3+}, Th^{4+}, Ce^{3+}, La^{3+}, Eu^{3+} and Tb^{3+}, c = 0.1 M, in room temperature).

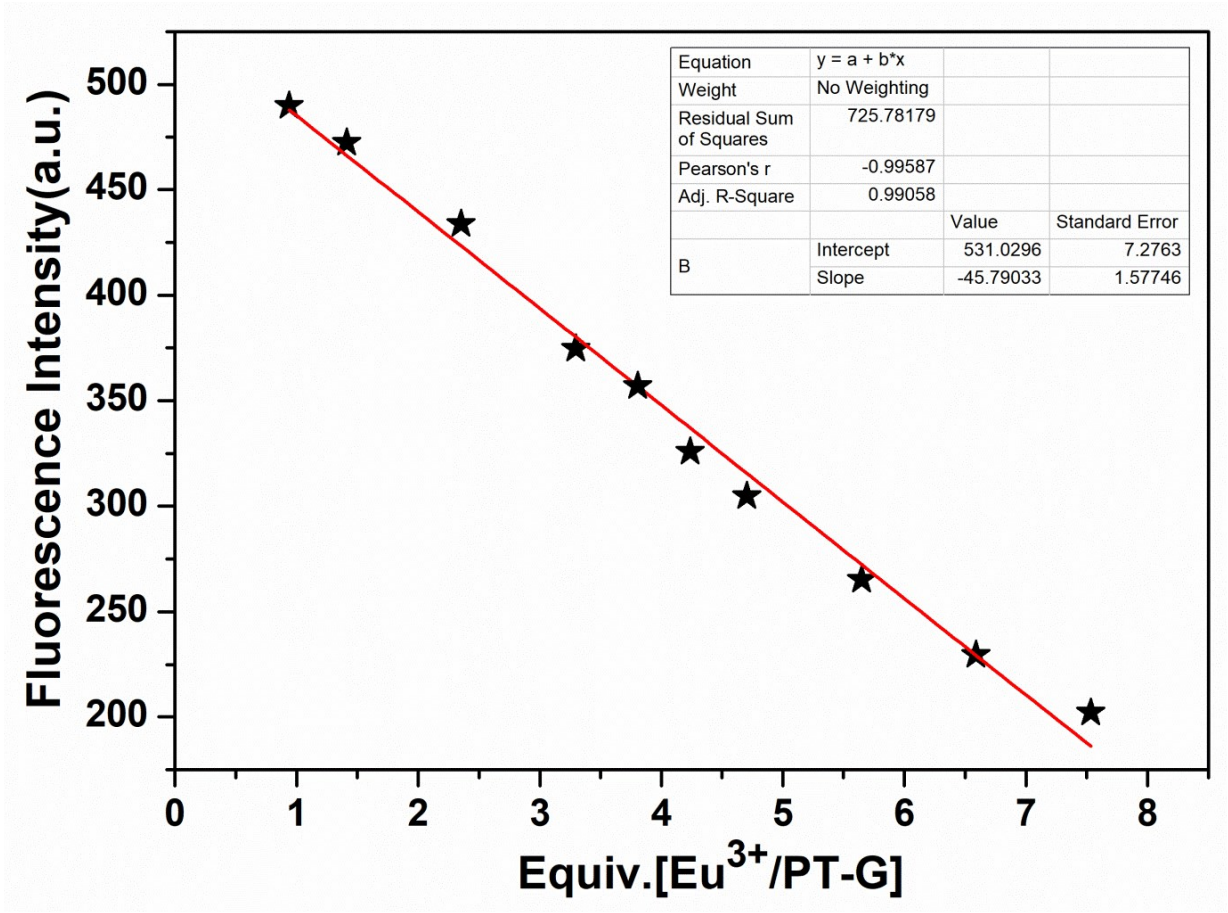

Figure S19. Photograph of the linear range for Eu^{3+}.

The result of the analysis as follows:

Linear Equation: Y= -45.79×X +531.02 R^2=0.99

S=4.58×10^7

$$\delta = \sqrt{\frac{\sum_{i=1}^{N}(F_i - \bar{F})2}{N-1}} = 1.58 \ (N=20)$$

LOD = K × δ/S =1.04×10^{-7} M (K=3)

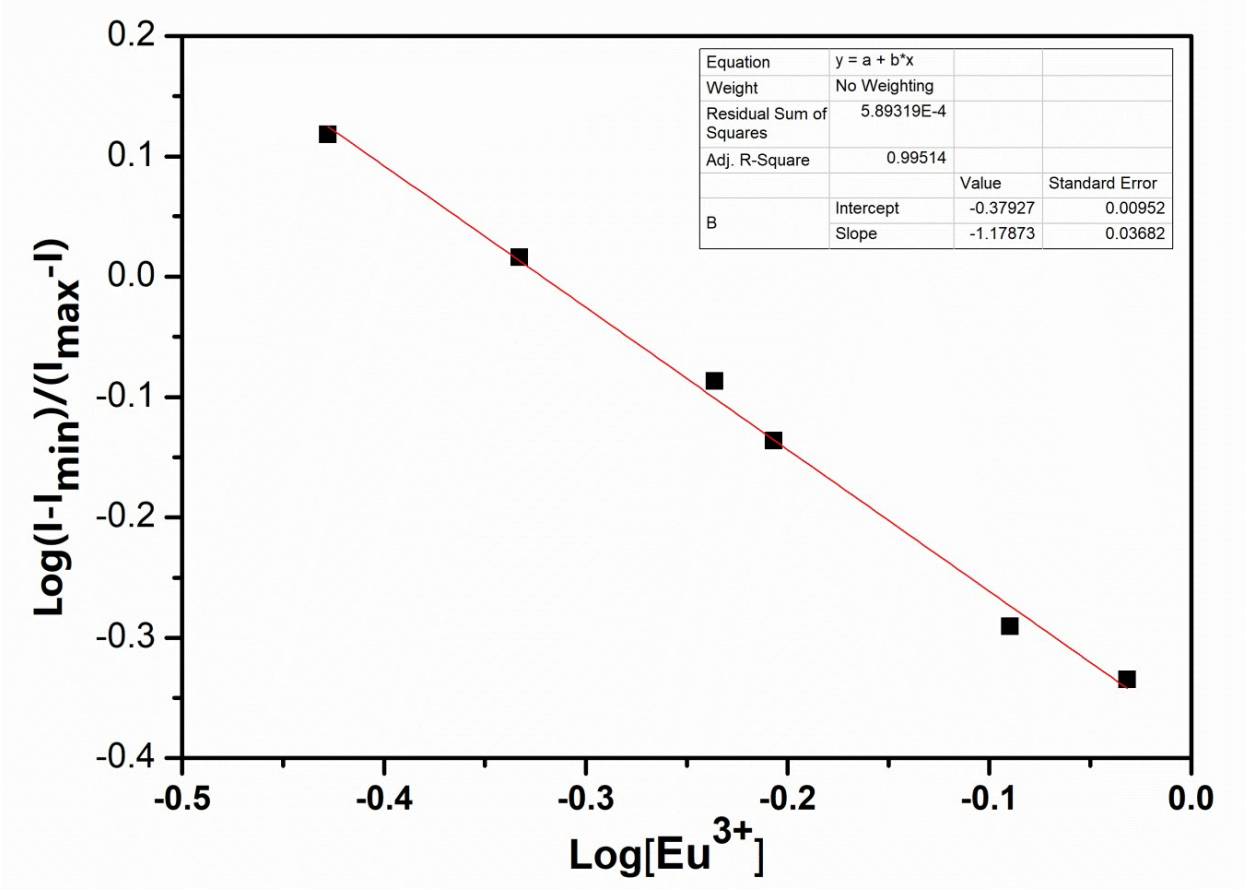

Figure S20. The association constant and complex ratio of **PT-G** and Eu^{3+} with fluorescent titration. Calculation formula: $$\log\frac{I-I_{min}}{I_{max}-I} = \log Ka + n\log[G]$$.

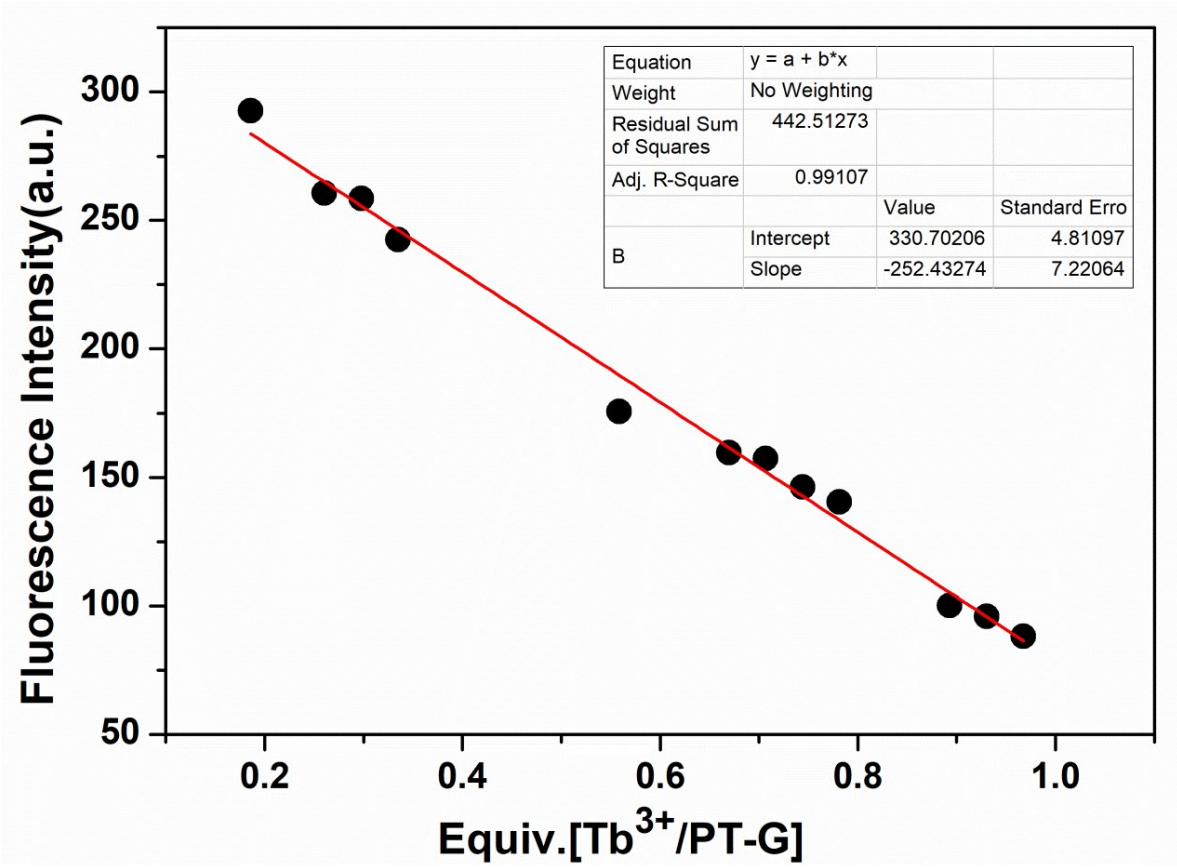

Figure S21. Photograph of the linear range for Tb^{3+}.

The result of the analysis as follows:

Linear Equation: Y= -252.43×X +330.70 R^2=0.99

S=2.52×10^8

$$\delta = \sqrt{\frac{\sum_{i=1}^{N}(F_i - \overline{F})2}{N-1}} = 1.77 \ (N=20)$$

LOD = K × δ/S =2.10×10^{-8} M (K=3)

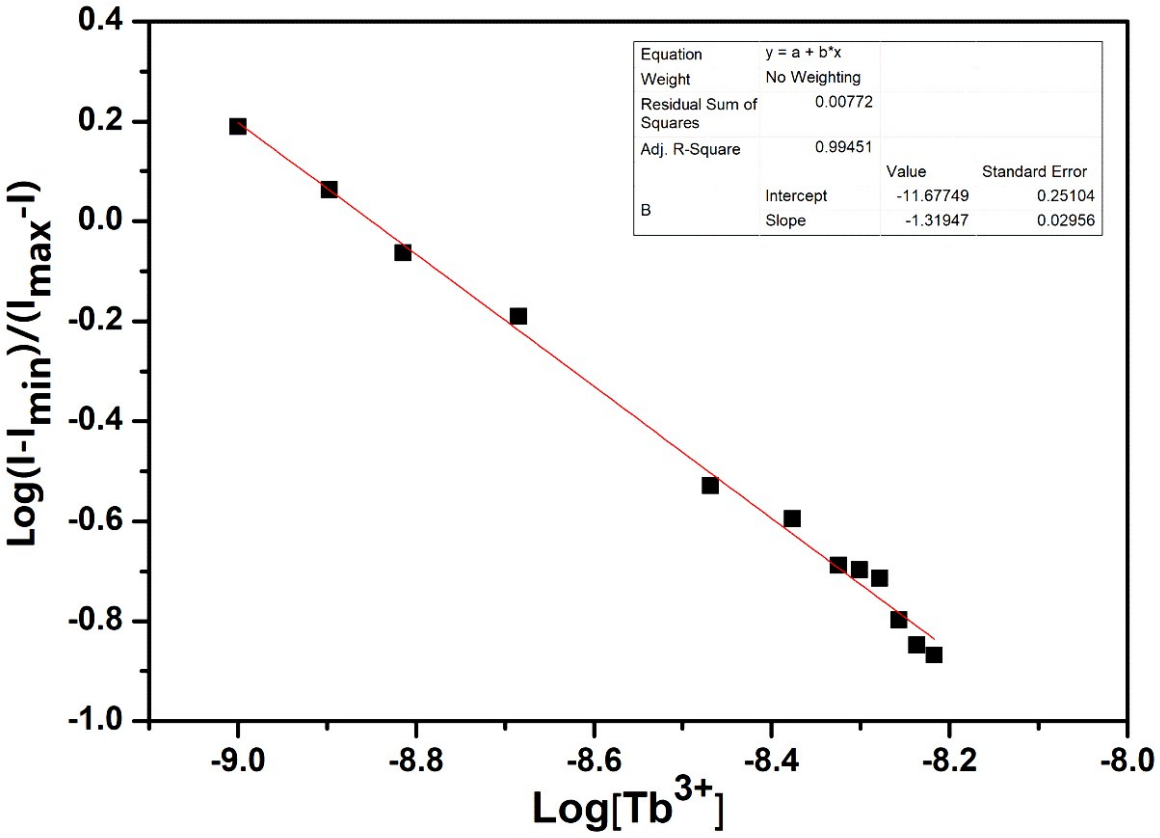

Figure S22. The association constant and complex ratio of **PT-G** and Tb^{3+} with fluorescent titration. Calculation formula: $$\log\frac{I-I_{min}}{I_{max}-I}=\log Ka+n\log[G]$$

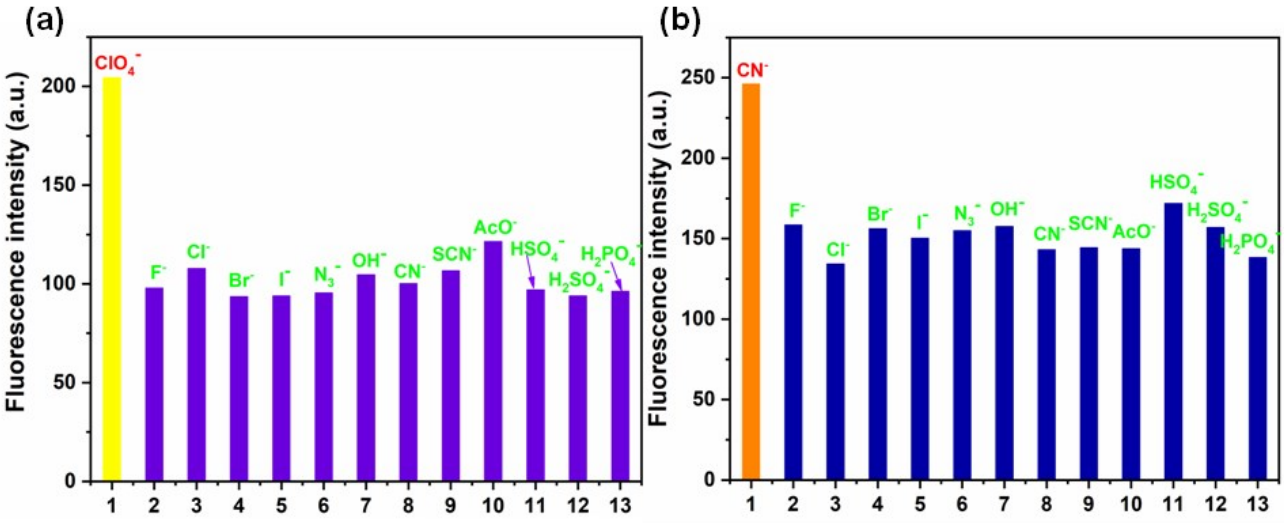

Figure S23. (a) Fluorescence spectrum responses of the **PT-GEu** (DMSO-H_2O (2: 1, v/v)) upon adding of various anions (ClO_4^-, F^-, Cl^-, Br^-, I^-, N_3^-, OH^-, CN^-, SCN^-, AcO^-, HSO_4^-,

$H_2SO_4^-$ and $H_2PO_4^-$, c = 0.1 M, in room temperature); (b) Fluorescence spectrum responses of the **PT-GTb** (DMSO-H_2O (2: 1, v/v)) upon adding of various anions (CN^-, F^-, Cl^-, Br^-, I^-, N_3^-, OH^-, SCN^-, AcO^-, HSO_4^-, $H_2SO_4^-$, ClO_4^- and $H_2PO_4^-$, c = 0.1 M, in room temperature).

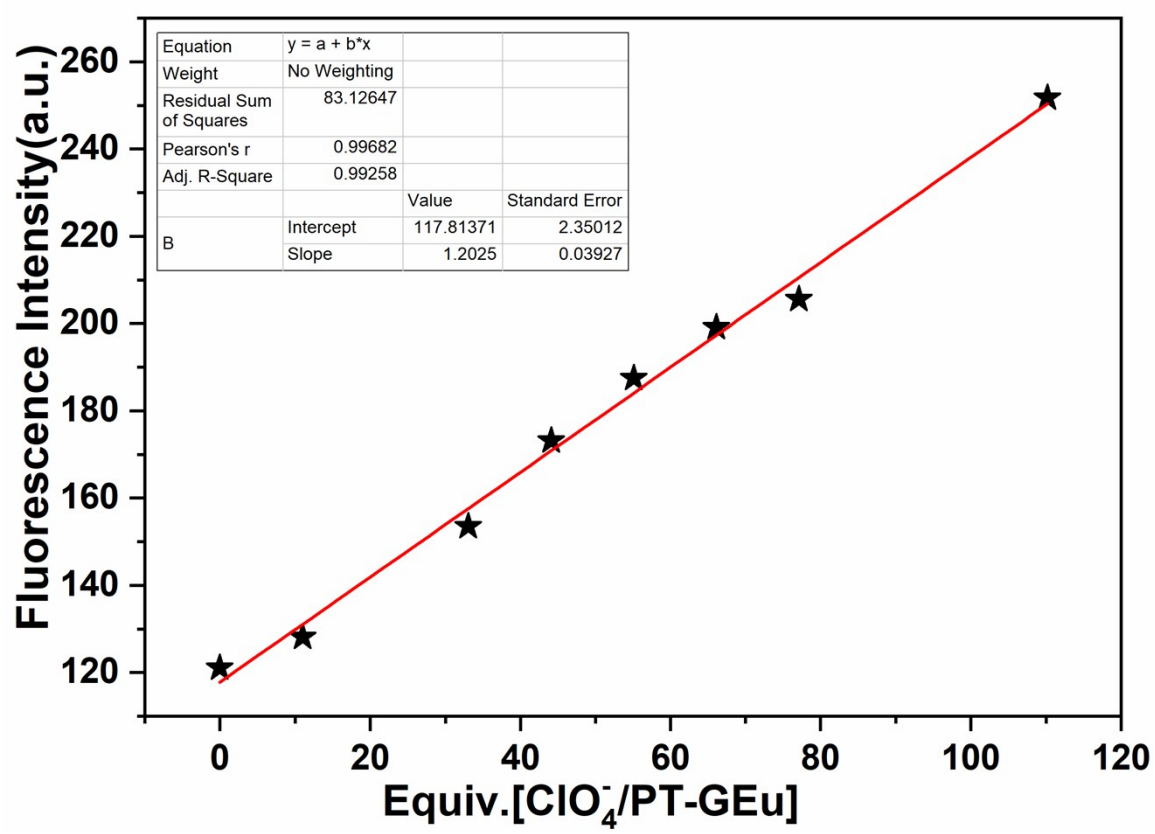

Figure S24. Photograph of the linear range for ClO_4^-.

The result of the analysis as follows:

Linear Equation: Y= 1.20 ×X + 117.81 R^2=0.99

S=1.20×10^6

$$\delta = \sqrt{\frac{\sum_{i=1}^{N}(F_i - \overline{F})2}{N-1}} = 1.35 \text{ (N=20)}$$

LOD = K × δ/S =3.36×10^{-6} M (K=3).

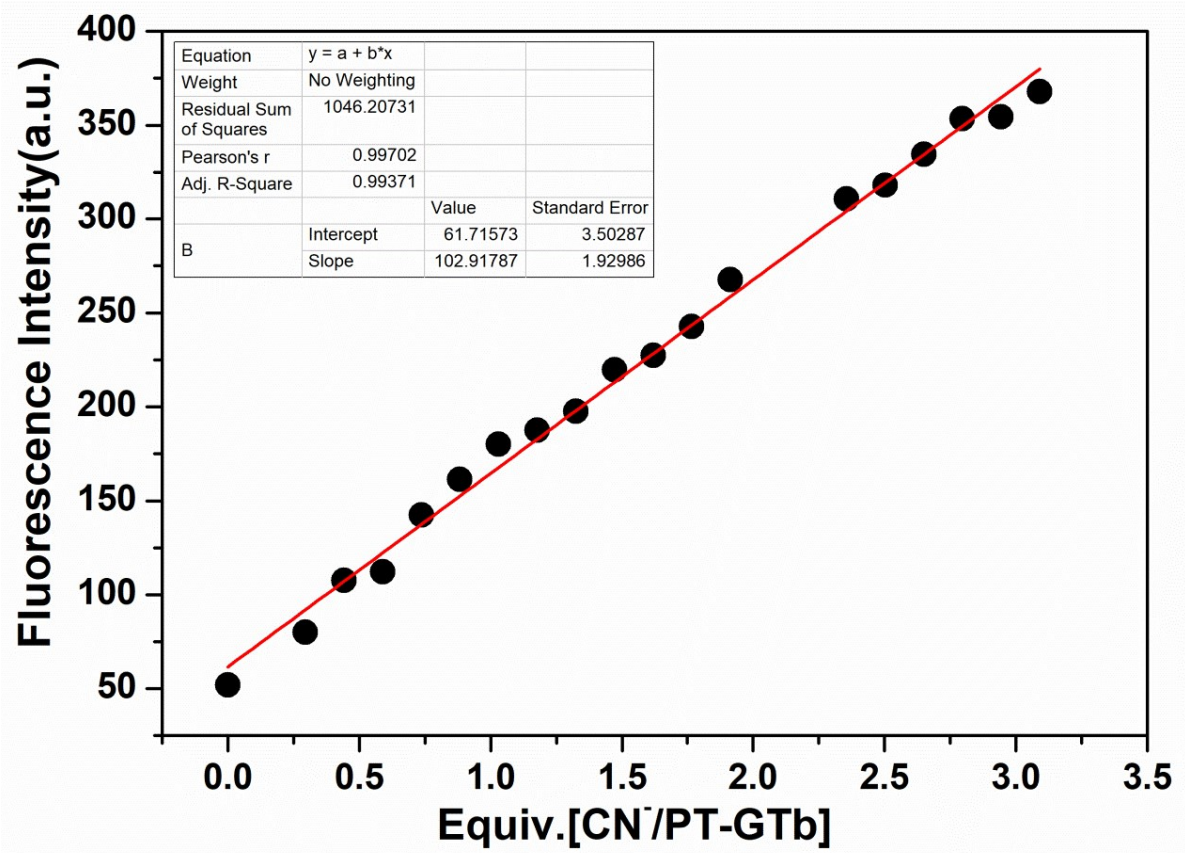

Figure S25. Photograph of the linear range for CN^-.

The result of the analysis as follows:

Linear Equation: $Y=102.92\times X + 61.72$ $R^2=0.99$

$S=1.03\times10^8$

$\delta=\sqrt{\frac{\sum_{i=1}^{N}(F_i-\bar{F})2}{N-1}}$ =2.05 (N=20)

$LOD = K \times \delta/S = 5.96\times10^{-8}$ M (K=3)

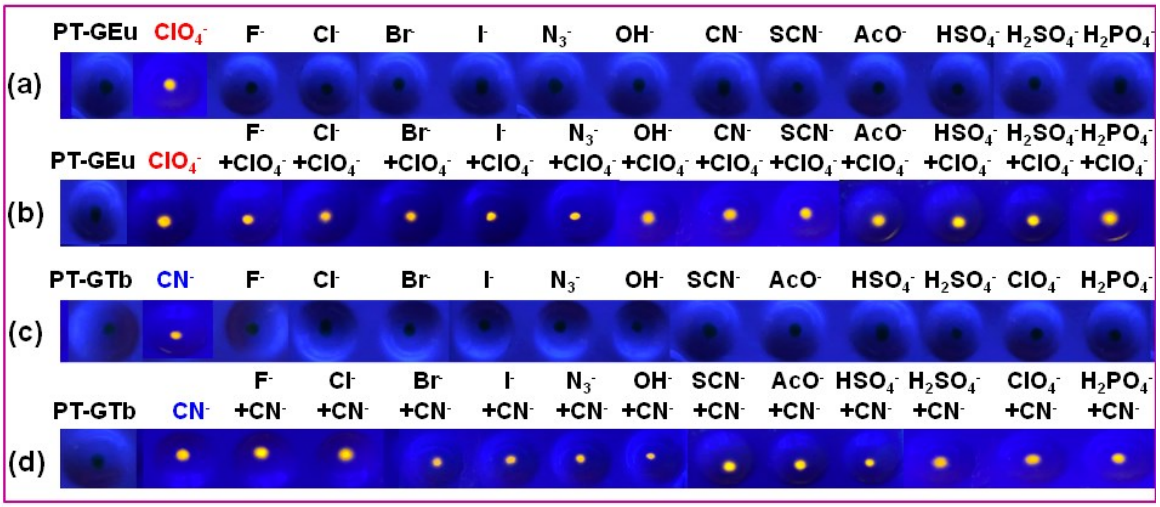

Figure S26. The control experiments: (a) **PT-GEu** and **PT-GEu** treated by water solutions of various anions (F^-, Cl^-, Br^-, I^-, N_3^-, OH^-, CN^-, SCN^-, AcO^-, HSO_4^-, $H_2SO_4^-$, ClO_4^- and $H_2PO_4^-$); (b) **PT-GEu** and **PT-GEu** contained water solutions of various anions (F^-, Cl^-, Br^-, I^-, N_3^-, OH^-, CN^-, SCN^-, AcO^-, HSO_4^-, $H_2SO_4^-$ and $H_2PO_4^-$) treated by water solution of ClO_4^-. (c) **PT-GTb** and **PT-GTb** treated by water solutions of various anions (F^-, Cl^-, Br^-, I^-, N_3^-, OH^-, CN^-, SCN^-, AcO^-, HSO_4^-, $H_2SO_4^-$, ClO_4^- and $H_2PO_4^-$); (d) **PT-GTb** and **PT-GTb** contained water solutions of various anions (F^-, Cl^-, Br^-, I^-, N_3^-, OH^-, SCN^-, AcO^-, HSO_4^-, $H_2SO_4^-$, ClO_4^- and $H_2PO_4^-$) treated by water solution of CN^-.

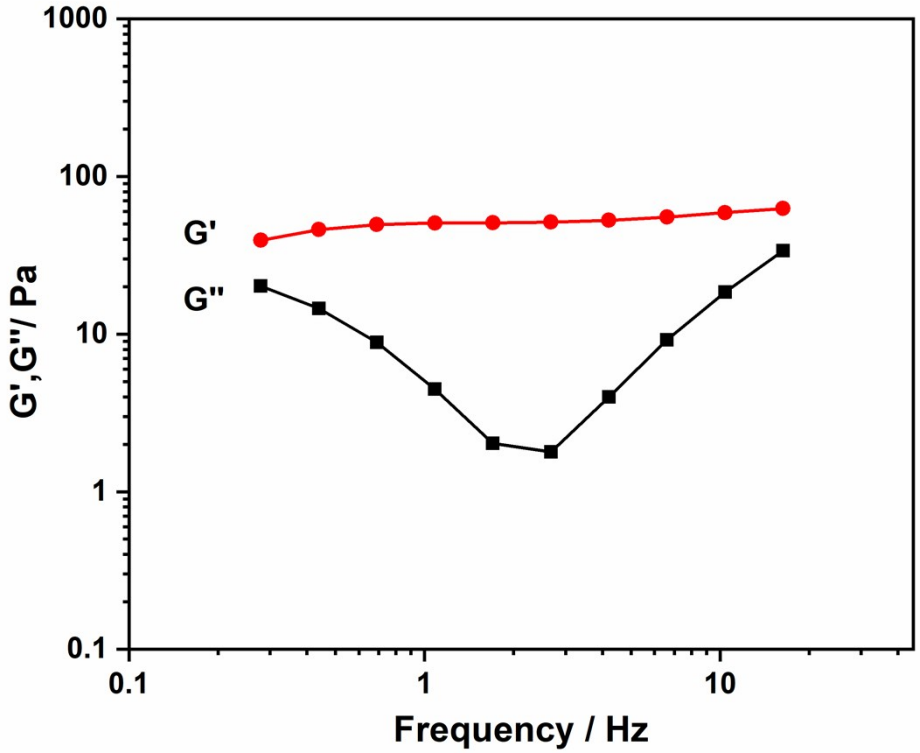

Figure S27. Frequency-dependent elastic (or storage) modulus G' and viscous (or loss) modulus G'' of the supramolecular hydrogel for **PT-G**.

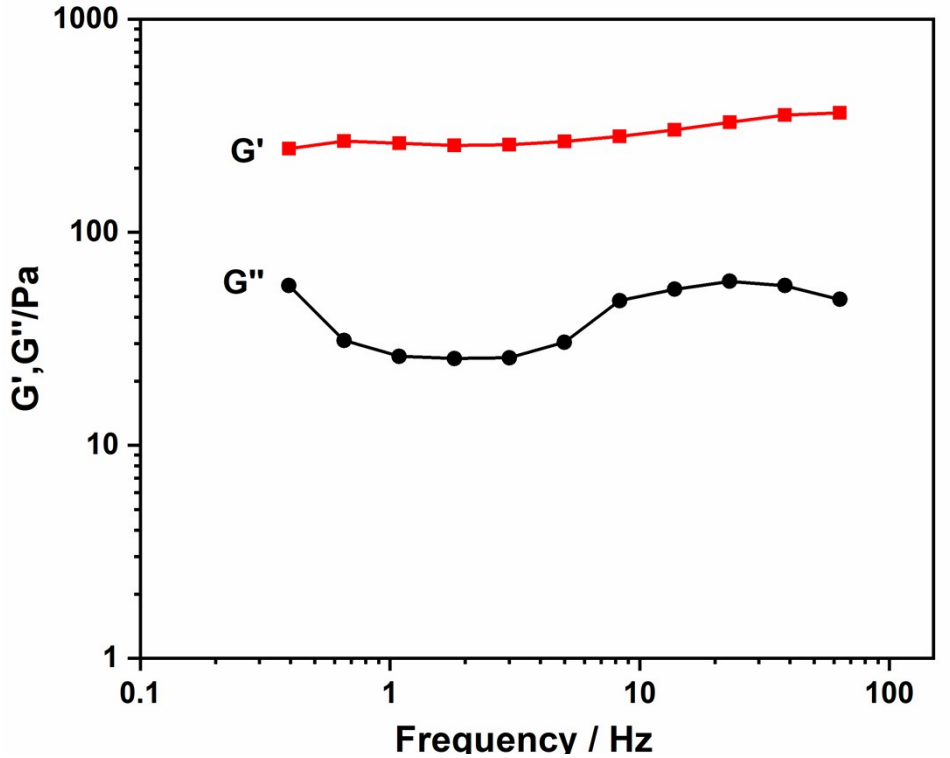

Figure S28. Frequency-dependent elastic (or storage) modulus G' and viscous (or loss) modulus G'' of the supramolecular hydrogel for **PT-GEu.**

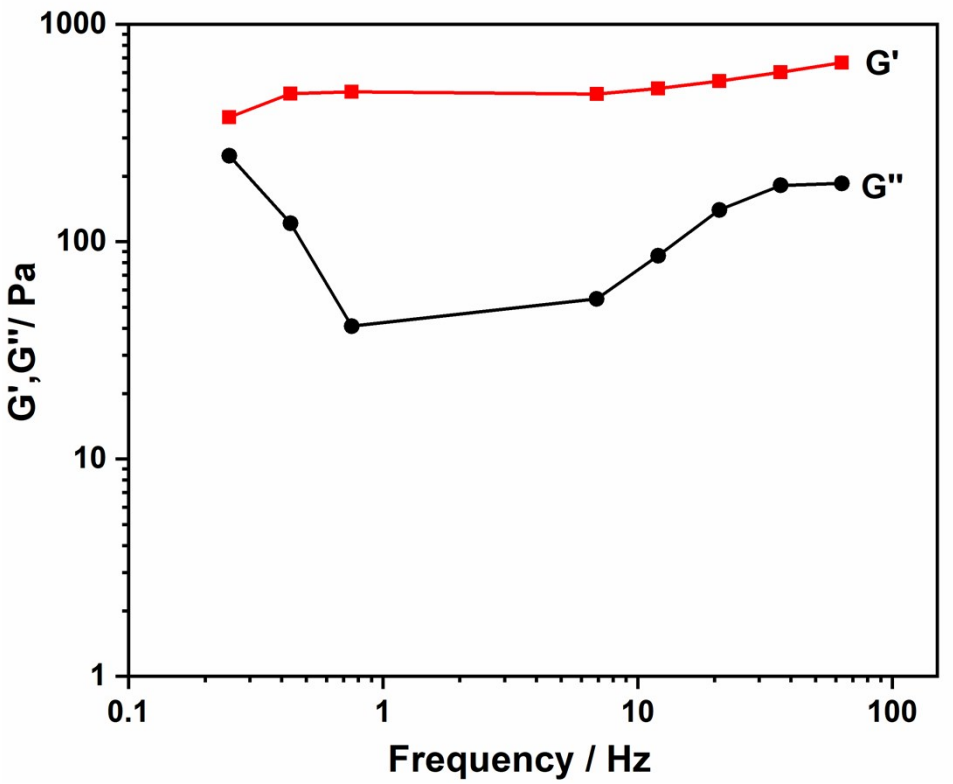

Figure S29. Frequency-dependent elastic (or storage) modulus G' and viscous (or loss) modulus G'' of the supramolecular hydrogel for **PT-GTb**.

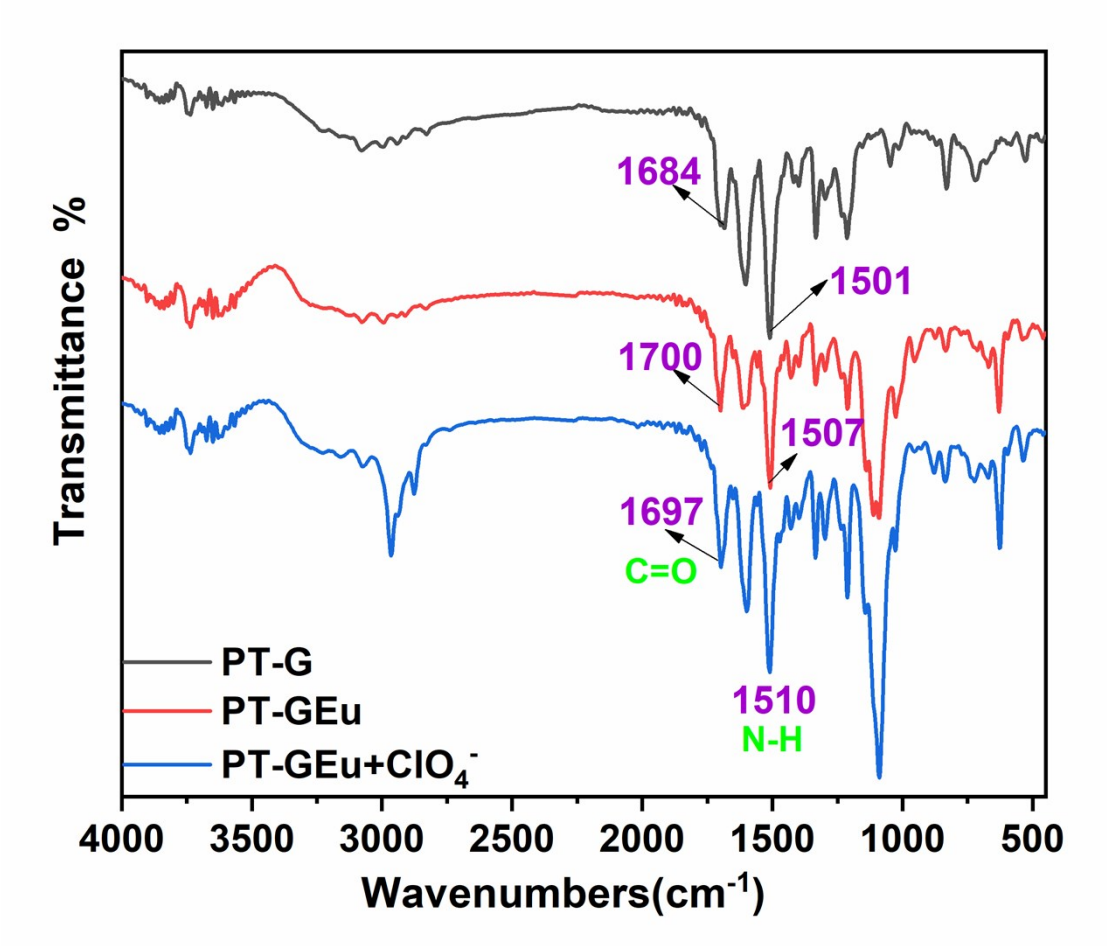

Figure S30. FT-IR spectra of the **PT-G**, **PT-GEu** and **PT-GEu+ClO_4^-.**

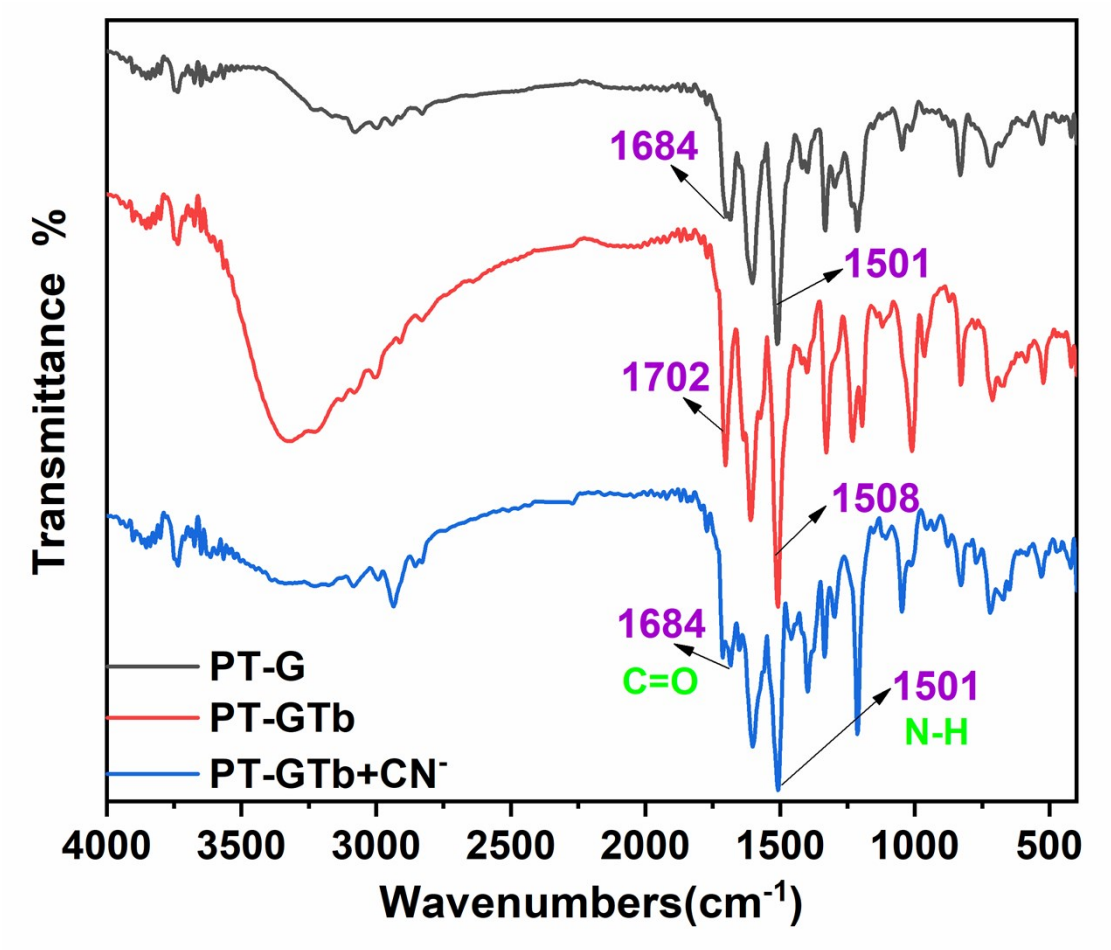

Figure S31. FT-IR spectra of the **PT-G**, **PT-GTb** and **PT-GTb+CN$^-$**.

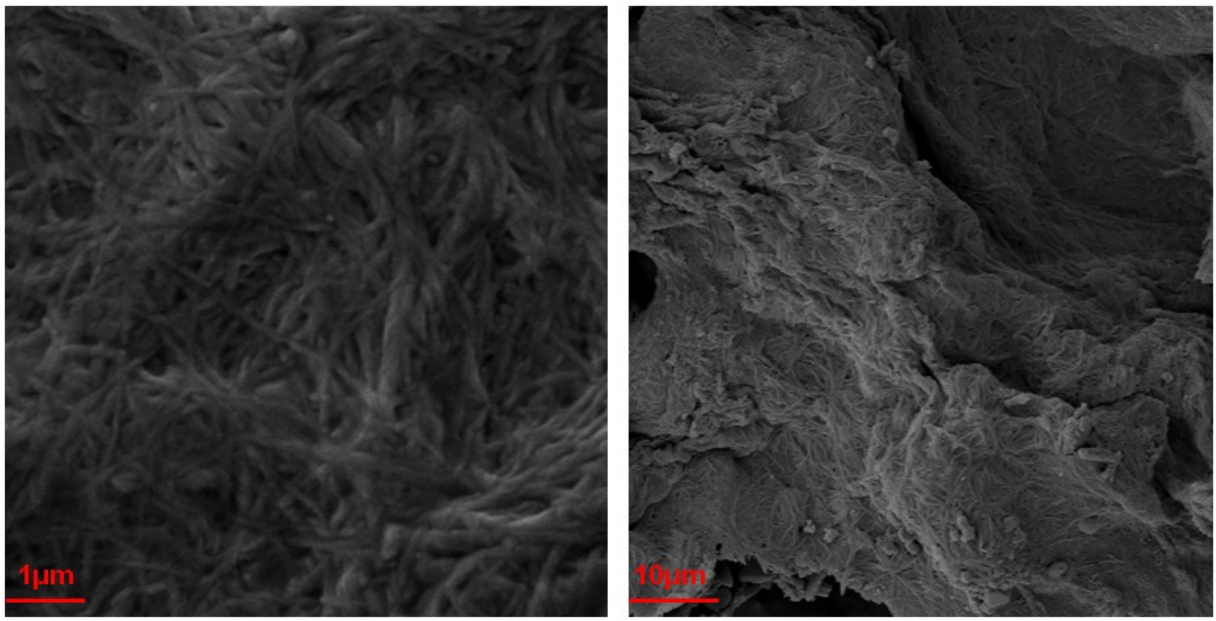

Figure S32. SEM images of (f) xerogel **PT-GTb**, (g) xerogel **PT-GTb+CN$^-$.**

Figure S33. Fluorescence colors changes (under the UV lamp, at λ_{ex} = 365 nm) of the **PT-G** and **PT-GEu-**based test kits after addition of different concentration Eu^{3+} and ClO_4^- (from 0 M to 0.1 M).

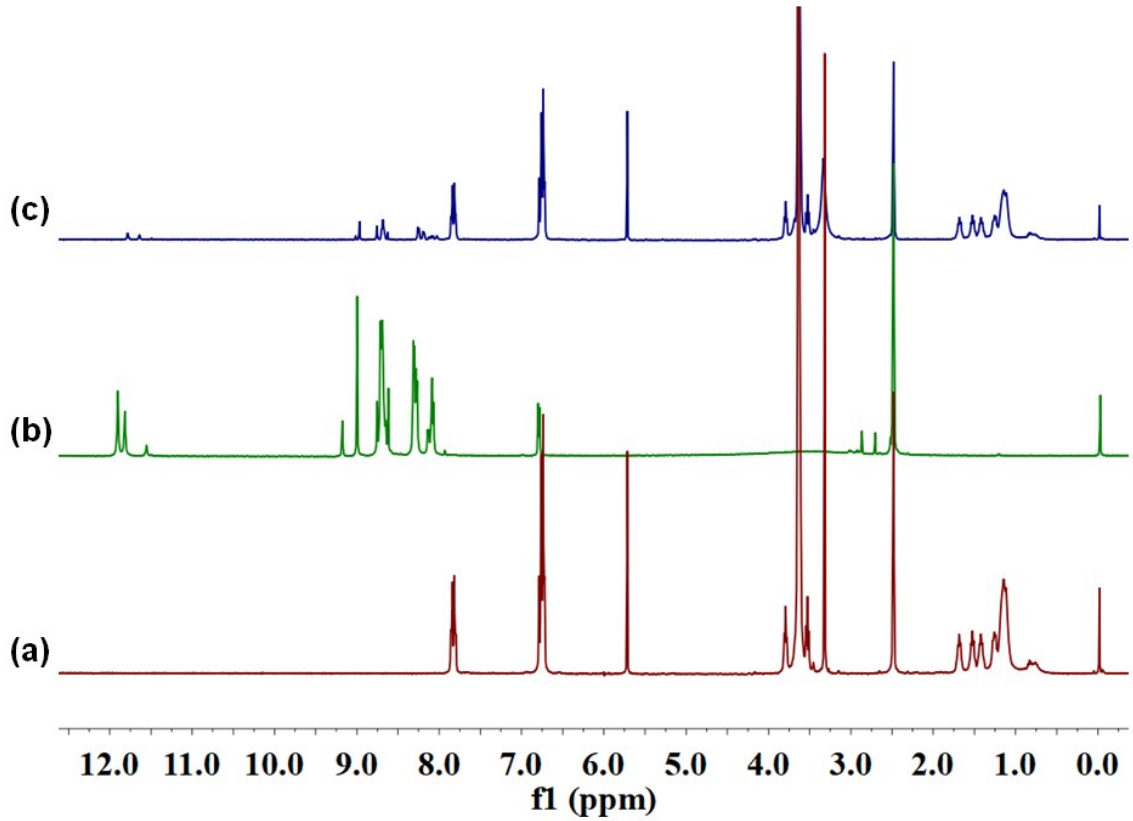

Figure S34. Complete host-guest ^{1}H NMR spectra of (a) free **PM,** (b) free **TH**, (c) **PM⊂TH** 3.0 equiv. in (DMSO-d_6).

3. Supplementary table

Table S1. Gelation Properties of PT-G in Different Organic Solvents.

Entry	Solvent	State[a]	CGC[b](%)	Tgel[c](^{o}C,wt%)
1	water	P	\	\
2	acetone	p	\	\
3	methanol	P	\	\
4	ethanol	p	\	\
5	isopropanol	p	\	\
6	isopentanol	p	\	\
7	acetonitrile	P	\	\
8	THF	S	\	\
9	DMF	S	\	\
10	DMF + H_2O	P	\	\
11	DMSO	S	\	\
12	DMSO + H_2O	G	3.33%	57 ^{o}C
13	CCl_4	P	\	\
14	n-hexane	p	\	\
15	ethanediol	P	\	\
16	tert-butylalcohol	P	\	\
17	CH_2Cl_2	S	\	\
18	$CHCl_3$	S	\	\
19	CH_2ClCH_2Cl	P	\	\
20	petroleum ether	P	\	\
21	ethyl acetate	P	\	\
22	n-propanol	p	\	\
23	n-butyl alcohol	p	\	\
24	cyclohexanol	S	\	\
25	n-hexanol	p	\	\
26	propanetriol	—	\	\

[a] G, P and S denote gelation, precipitation and solution, respectively.

[b] The critical gelation concentration (wt%, 10mg/ml = 1.0%).

[c] The gelation temperature (^{o}C).

Table S2. The HPIC date of PT-GTb and PT-GEu with ClO_4^- and CN^-.

Ion	Initial concentration (M)	Residual concentration (M)	Absorbing rate %
ClO_4^-	1×10^{-4} M	6.67×10^{-6} M	93.33%
CN^-	1×10^{-4} M	7.14×10^{-6} M	92.86%

Calculation method of adsorption percentage:

$$Adsorption\ percentage(\%) = \left(1 - \frac{C_R \times V_R}{C_I \times V_I}\right) \times 100\%$$

(State: C_R is the residual concentration of ClO_4^- and CN^-, C_I is the initial concentration of ClO_4^- and CN^-, $V_R=V_I$).

4.**References**

[1] You-Ming Zhang, Wei Zhu, Xiao-Juan Huang, Wen-Juan Qu, Jun-Xia He, Hu Fang, Hong Yao, Tai-Bao Wei, and Qi Lin, *ACS Sustainable Chem. Eng.*, 2018, **6**, 16597-16606.

[2] Yan-Qing Fan, Juan Liu, Yan-Yan Chen, Xiao-Wen Guan, Jiao Wang, Hong Yao, You-Ming Zhang, Tai-Bao Wei and Qi Lin, *J. Mater. Chem. C*, 2018, **6**, 13331.